Performance Evaluation of Constant Envelope OFDM working in 60 GHz Band

Achala Deshmukh [#1], Shrikant Bodhe[*2]

[#] Electronics and Telecommunication Engg. Department, Sinhgad College of Engineering, Pune University
c-403, Kakade City, Karve Nagar, Karve Road, Pune
Maharashtra, India
[*] Principal, College of Engineering, Pandharpur
Maharashtra, India
Director, Bosh Technologies, Pune
Maharashtra, India

[1] achala.deshmukh@gmail.com
[3] skbodhe@gmail.com

***Abstract*— The 60 GHz band is of much interest since this is the band in which a massive amount of spectral space (5 GHz) has been allocated unlicensed worldwide for dense wireless local communications. OFDM has gained much popularity in the field of wireless communication because of its ability to transfer the data at higher rate, high bandwidth efficiency and its robustness with regard to multipath and delay. But the major hurdle is high PAPR leading to inter-modulation distortion and out-of-band spectral growth. Constant envelope OFDM transforms the OFDM signal, to a signal with nearly zero dB PAPR. The PAPR performance of conventional OFDM system improves with constant envelope OFDM system.**

CE OFDM scheme provides PAPR to 0 dB; this paper analyzes the performance of CE OFDM on grounds of BER. A constant envelope OFDM system is considered for calculating bit error rate with additive white Gaussian noise (AWGN) channel and Saleh-Valenzuela (SV) channel model at 60 GHz. The BER is calculated for signalling format BPSK and the performance of CE OFDM is analyzed at 60 GHz

Keyword- OFDM (Orthogonal Frequency Division Multiplexing), PAPR (Peak-to-Average Power Ratio), constant envelope OFDM (CE OFDM)

I. INTRODUCTION

There is huge rise in demand from broadband wireless communication network systems to provide flexible high data-rate services. These high data-rate services need very high signal quality and therefore depend a lot on the wireless channels. The channel bandwidth available is very scarce resource. Again it is difficult to utilize the bandwidth effectively unless efficient techniques are employed. The wireless channel is characterized by impairments such as fading, shadowing and multi-user interference which highly degrades the system performance.

OFDM is a parallel-data-transmission technique, which reduces the influence of multipath fading and supports high data-rate links without requiring conventional equalization techniques [5]. OFDM is a special case of multicarrier transmission, where a single data stream is transmitted over a number of lower-rate subcarriers. OFDM is robust against narrowband interference because such interference affects only a small percentage of the sub carriers. OFDM is also robust against frequency-selective fading [3].

But the primary shortcoming of OFDM is that the modulated waveform has high amplitude fluctuations that produce large peak-to-average power ratio (PAPR). This high PAPR makes OFDM sensitive to nonlinear

distortion caused by the transmitter's power amplifier. Without sufficient power backoff, the system suffers from spectral broadening, intermodulation distortion, and consequently performance degradation. These problems can be reduced by increasing the power amplifier backoff, but this result in reduced power amplifier efficiency [9, 18].

Different techniques had been used to mitigate PAPR problem. It includes distortion less and non-distortion less schemes. Distortion less scheme include coding techniques or tone reservation whereby data symbols are mapped to a subset of OFDM waveforms giving relatively low PAPR. Non-distortion less PAPR reduction schemes includes clipping/filtering and peak windowing [24], [25]. All these techniques provide different tradeoffs such as increased complexity, reduced spectral efficiency, and performance degradation. An alternative approach to mitigate the PAPR problem is based on signal transformation. This technique is elaborated here which involves a signal transformation prior to amplification and an inverse transformation at the receiver prior to demodulation.

The signal transformation technique converts these variations in peak power and average power to a constant envelope like signal, hence called as Constant envelope OFDM (CE OFDM) system. In CE OFDM the OFDM signal is transformed with phase modulation, to a signal designed for efficient power amplification. At the receiver, the inverse transformation i.e. phase demodulation is applied prior to the conventional OFDM demodulator.

The CE OFDM system shares many of the functional blocks same as the conventional OFDM system. Thus an existing OFDM system can provide an additional CE OFDM mode with relative ease. The main difference in conventional OFDM system and CE OFDM system is that of the signal transformation achieved through phase modulation and phase demodulation.

Recent developments in wireless communications are being driven primarily by the increased demands for radio bandwidth. The 60 GHz band have a massive amount of spectral space (5 GHz), which has been allocated worldwide for dense wireless local communications. At this frequency band the specific attenuation due to atmospheric oxygen is 10–15 dB/km, (precisely 14.7 dB at 60 GHz) which makes the 60 GHz band unsuitable for long-range (greater than 2 km). For indoor environment distance is considered less than 50 m, therefore 10-15 dB/km attenuation does not carry much significant impact on the performance of communication system working in this band. Thus, there is 6 GHz (58 to 64 GHz) bandwidth available with specific attenuation in excess of 10 dB. The major reason for the interest in 60 GHz band is the huge unlicensed bandwidth. The range of unlicensed frequencies available is different in each country. This makes the 60 GHz band of utmost interest for all kinds of short-range wireless communications [28].

The power amplifier efficiency for mobile battery-powered devices is particularly an issue due to limited power resources. Efficient amplification is also a critical component to future systems operating in the unlicensed 60 GHz band [21]. Thus reducing the effect of peak-to-average power ratio (PAPR) is of importance to industrial and research communities. [22], [23].

.

II. CONSTANT ENVELOPE OFDM SYSTEM

An OFDM signal consists of a number of independently modulated subcarriers. But the multiple subcarriers are overlapped so that they occupy nearly half of the spectrum required by the conventional multicarrier system. The subcarriers are overlapping each other but in such a way that not a single subcarrier will cause interference to other subcarrier. The main advantage of OFDM is the utilization of the bandwidth effectively and efficiently. This is achieved by placing the subcarriers orthogonally with respect to each other. When N such subcarriers are added up coherently, they produce signal with a peak power N times the average power.

CE OFDM uses a completely different technique of signal transformation for reduction in PAPR. This technique includes phase modulation at the transmitter and phase demodulation at the receiver. Phase modulation transforms the amplitude variations in OFDM signal into a constant amplitude signal thereby reducing the vast difference between the peak power and average power. This generates a signal with a constant envelope.

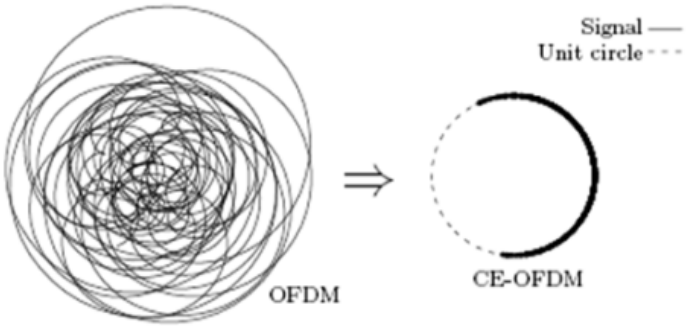

Fig. 1: CE OFDM waveform mapping

The CE OFDM is mapping of the OFDM signal to a unit circle [17], as depicted in Fig 1. The instantaneous power of the resulting signal is constant. For the CE OFDM signal, the peak and average powers are the same, thus the PAPR is *0* dB.

A. CE OFDM Transmitter:

The transmitter of the CE OFDM scheme is shown in the Fig 2. The input data is firstly mapped with a digital modulator and then converted from a serial stream to parallel sets. Each set of data contains one symbol, *Si*, for each subcarrier. During each *T*-second block interval, an *N*-DFT point Inverse Discrete Fourier Transform (IDFT) generates sum of orthogonal sub carriers $x[n]$ [10].

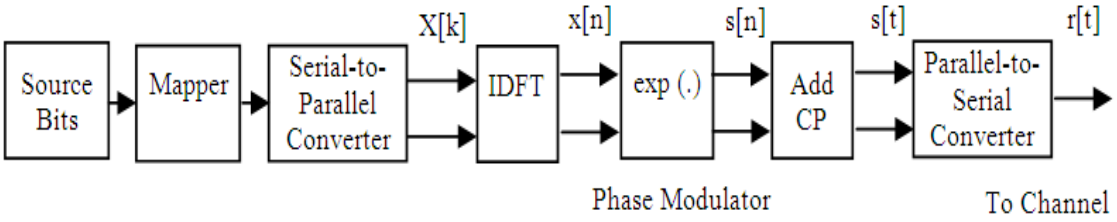

Fig. 2: CE OFDM System Model – Transmitter

Then, $x[n]$ which is a high PAPR OFDM sequence is passed through a phase modulator to obtain the *0* dB PAPR sequence [18] indicated as $exp\,(.)$ in Fig.2. The cyclic prefix (CP) is appended to $s[n]$ before transmission of the signal. Cyclic prefix is a crucial feature of OFDM used to combat the Inter-Symbol-Interference (ISI) and Inter-Channel-Interference (ICI) introduced by the multi-path propagation through the channel through which the signal is propagated [4]. The basic idea is to replicate part of the OFDM symbol from the back-to-the-front to create a guard period.

During each *T*-second block interval, an *N*- point Inverse Discrete Fourier Transform (IDFT) calculates a block of time samples $x[n]$. The sampling rate is therefore $F_0 = \frac{N_{DFT}}{T}$ [18]. To obtain a real-valued, oversampled OFDM sequence $x[n]$, the input to the IDFT is a conjugate symmetric, zero-padded data vector [6] as given in Eq.(1)

$$\left[0, X[1], X[2], \dots, X\left[N_{QAM}\right], \quad 0_{1\times N_{ZP,}} 0, X^*\left[N_{QAM}\right], \dots, X^*[2], X^*[1]\right] \qquad (1)$$

Where $\{X[K]\}_{K=1}^{N_{QAM}}$ is QAM data symbols, and $0_{1\times N_{ZP}}$ is an N_{ZP}-element row vector comprised of zeros. The IDFT size is thus $N_{DFT} = 2N_{QAM} + N_{ZP} + 2$. The zeros at index $K = 0$ and $K = N_{QAM} + N_{ZP} + 1$ are used to maintain conjugate symmetry, and the remaining N_{ZP} zeros achieve the effect of oversampling the time-domain sequence. The oversampling factor is defined as $C_{OS} = \frac{N_{DFT}}{N_{DFT-}\, N_{ZP}}$. Using this convention, the output of the IDFT is expressed as in Eq. (2), (3).

$$x[n] = \sum_{k=o}^{N_{DFT}-1} X[k] e^{j2\pi kn/N_{DFT}} \qquad (2)$$

$$x[n] = 2 \sum_{k=1}^{N_{QAM}} \Re\{X[k]\} \cos\left(\frac{2\pi kn}{N_{DFT}}\right) - \Im\{X[k]\} \sin\left(\frac{2\pi kn}{N_{DFT}}\right) \qquad (3)$$

Where $n = 0, 1, \dots, N_{DFT} - 1$ and $j = \sqrt{-1}$

Next, $x[n]$, which is a high PAPR OFDM sequence, is passed through a phase modulator to obtain *0* dB PAPR sequence as given in Eq. (4) where *C* is a scaling constant.

$$s[n] = e^{jC\, x[n]} \qquad (4)$$

Phase Modulation (PM) represents information as variations in the instantaneous phase of a carrier wave. If $\boldsymbol{c(t)}$ is the carrier given by Eq. (5)

$$\boldsymbol{c(t) = A_C \sin(\omega_c t + \varphi_c)} \qquad (\mathbf{5})$$

The phase modulated signal is as expressed in Eq. (6) when $m(t)$ is message signal.

$$y(t) = A_C \sin(\omega_c t + m(t)\, \varphi_c) \qquad (6)$$

The modulation index $m(t)$ is the key parameter that controls the signal space performance and the spectral properties of CE OFDM.

In the above block diagram the $exp(.)$ block acts as a phase modulator which actually achieves PAPR reduction. Further N_{CP} sample cyclic prefix (CP) is appended to $\{s[n]\}$ to obtain $\{s[n]\}_{n=-N_{CP}}^{N_{DFT}-1}$ where $s[n] = s[N_{DFT} + n]$ and $n = N_{CP} - 1, \dots, -2, -1$. Parallel-to-Serial Converter creates the OFDM signal by sequentially outputting the time domain samples. The low pass equivalent representation of the amplified CE OFDM signal is given as Eq. (7) for $-T_{CP} \le t < T$

$$s[n] = A\, e^{j[2\pi h m(t) + \theta]} \qquad (7)$$

Where A is the signal amplitude and θ is an arbitrary phase offset which may be used as a design parameter to achieve phase modulation. The cyclic prefix duration is $T_{CP} = \frac{N_{CP}}{F_0}$ and the block duration is $T = \frac{N_{DFT}}{F_0}$. The information bearing message signal $m(t)$ is a real-valued OFDM waveform having the same form as Eq. (3) as given in Eq. (8) $-T_{CP} \leq t < T$

$$m(t) = C \sum_{k=1}^{N_{QAM}} \Re\{X[k]\} \cos\left(\frac{2\pi kt}{T}\right) - \Im\{X[k]\} \sin\left(\frac{2\pi kt}{T}\right) \qquad (8)$$

Where C is a constant. Therefore, the phase modulating OFDM signal is comprised of $N = 2N_{QAM}$ subcarriers each modulated by $M = \sqrt{M_{QAM}}$ ary data symbols.

It is convenient to define the message signal as Eq. (9)

$$m(t) = C_{norm} \sum_{k=1}^{N} I[k]\, qk(t) \qquad (9)$$

$$\text{Where } I[k] = \begin{cases} \Re\{X[k]\}, & k = 1, 2, \dots, N_{QAM} \\ -\Im\{X[k - N_{QAM}]\} & k = N_{QAM} + 1, \dots, N \end{cases} \qquad (10)$$

Where $I[k] \in \{\pm 1, \pm 3, \dots, \pm(M-1)\}$ are M-PAM data symbols, and

$$q_k(t) = \begin{cases} \cos\left(\frac{2\pi kt}{T}\right), & k = 1, 2, \dots., N_{QAM} \\ \sin\left(\frac{2\,\pi[k - N_{QAM}]t}{T}\right), & k = N_{QAM} + 1, \dots., N \end{cases} \qquad (11)$$

Eq. (11) is the subcarriers. C_{norm} as expressed in Eq.(14), is a constant used to normalize the variance of the message signal $(\sigma_m^2 = 1)$ thus making the variance of the phase signal as given in Eq. (12), (13)

$$\varphi(t) = 2\pi h m(t) \qquad (12)$$

$$\sigma_\varphi^2 = (2\pi h)^2 \qquad (13)$$

where h is the modulation index. This is achieved by establishing Eq. (14)

$$C_{norm} = \sqrt{\frac{2}{(N\sigma_I^2)}} \qquad (14)$$

Where $\sigma_I^2 = (M^2 - 1)/3$, and it is the variance of the independent and identically distributed data symbols. The subcarriers are centred at the frequencies $\pm\ i/T$ Hz, where $i = 1, 2, \dots, N/2,$ so an effective double-sided bandwidth of the message signal is defined as $W \equiv \frac{N}{T}\ Hz$. The bandwidth of $s(t)$ is lower bounded by W Hz, and a function of the modulation index.

The bandwidth of CE OFDM signal is given by Eq. (15)

$$B = max(2\pi h, 1)\, W \quad Hz \qquad (15)$$

The Bit rate is given in Eq. (16) and the Spectral efficiency is given in Eq. (17)

$$R = N\ log_2 \frac{M}{T} \quad bit/\sec \qquad (16)$$

$$S = \frac{R}{B} = \frac{log_2\ M}{max(2\pi h, 1)} \quad \frac{bps}{Hz} \qquad (17)$$

The Baseband representation of the received signal is as in Eq. (18)

$$r(t) = \int_0^{\tau_{max}} y(\tau, t)\ s(t-\tau)\ d\tau\ + w(t) \qquad (18)$$

where $y(\tau, t)$ is the channel impulse response with maximum propagation delay τ_{max} , and $w(t)$ is complex-valued Gaussian noise with a power spectral density $\Phi_{ww}(f) = N_0$ over the effective bandwidth of $s(t)$.

B. CE OFDM Receiver:

At the receiver end as shown in the Fig. 3, the cyclic prefix samples are discarded firstly and the remaining samples $r[n]$ are processed [17].

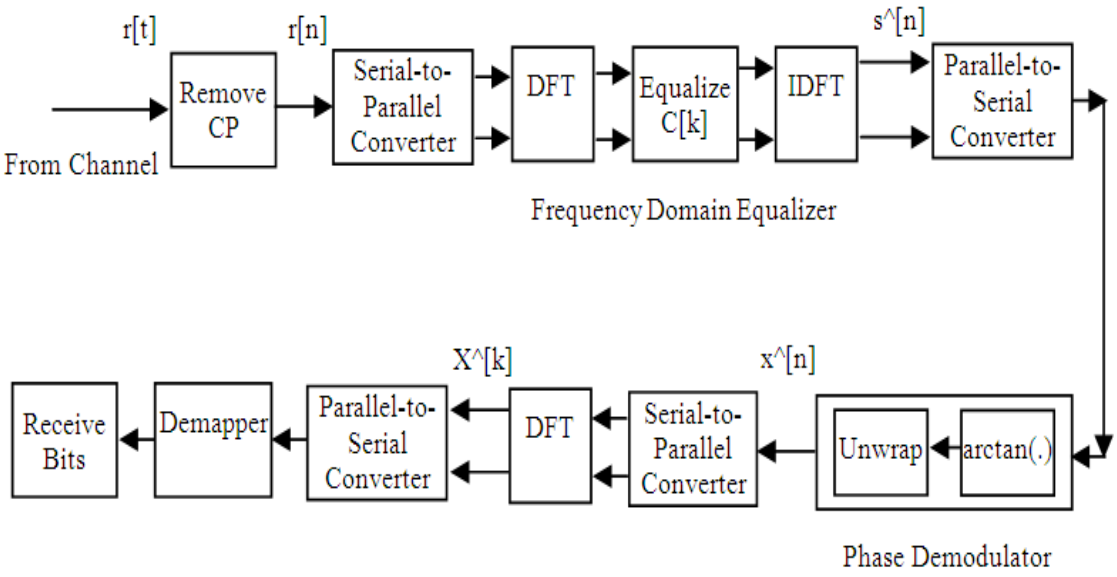

Fig. 3: CE OFDM System Model – Receiver

At the phase demodulator block, the phase is extracted by taking the inverse tangent [12] of the quadrature baseband components using the $arctan(.)$ block. This is followed by a phase unwrapper to obtain the phase demodulated signal $x^{\wedge}[n]$. The phase estimate from the phase demodulator is confined to the 2π range from $(-\pi\ to\ +\pi)$. The original transmit phase that deviates outside the $-\pi$ to $+\pi$ range is wrapped to within this range. Phase wrapping is more frequent for larger modulation indices whereby the large OFDM signal peaks result in large fluctuations in the CE OFDM transmit phase.

The output of the phase demodulator is in serial form which is converted to parallel and then processed by the OFDM demodulator which consists of the *N* correlators, one corresponding to each subcarrier. This correlator bank is implemented in practice with the Discrete Fourier Transform resulting in $X[k]$. The data in serial from is demodulated by a symbol demapper that yields the received bits.

Thus, the transmitter achieves reduction in PAPR by modulating the phase of the signal, to nearly *0* dB after conventional OFDM modulation. At the receiver side, phase demodulation is done first followed by the conventional OFDM demodulation. Thus, the signal transformation technique works.

The received signal obtains the samples as in Eq. (19)

$$r[n] \equiv r(n/F_0) = \sum_{l=0}^{L-1} h[l]s[n-1] + w[n] \qquad (19)$$

For $n = -N_{CP}, \ldots, N_{DFT} - 1$ and $w[n] \equiv w(n/F_0)$. The cyclic prefix duration is designed such that $N_{CP} \geq L$.

The Frequency Domain Equalizer (FDE) provides a simple technique to mitigate the distortion due to a frequency selective channel [17]. The use of a cyclic prefix in CE OFDM (like OFDM) not only prevents Inter-block-Interference (IBI) but also transforms the linear convolutions common in time-dispersive channels into circular convolutions. These circular convolutions in the time domain are equivalent to multiplication in the frequency domain. This characteristic is fundamental to the implementation of the frequency domain equalizer and allows the use of the DFT/IDFT pair.

Frequency domain equalization is accomplished in three main steps on a per block basis [15]. The received time signal is first transformed into the frequency domain by simple application of the FFT as given in Eq. (20).

$$R_k = \sum_{m=0}^{N_{FFT}-1} r_m \; e^{-j\left(\frac{2\pi k}{N_{FFT}}\right)m} \qquad (20)$$

$r_m = r[m] = r(mT_0)$ is the m^{th} time sample of the received time signal sampled at rate $f_s = k/T_s$ and T_o is the sampling period. Here R_k represents the frequency component of the received signal at frequency $f_s = k/T_s$ and T_s is symbol period.

The frequency domain equalizer consists of a single tap equalizer with a complex tap at each of the discrete frequency components, f_k obtained after DFT. Each received signal frequency component is multiplied by a complex coefficient (tap) as in Eq. (21).

$$X_k = R_k \, C_k \qquad (21)$$

Where C_k is the coefficient that attempts to invert the channel response at the frequency, $f_s = k/T_s$ while X_k represents the equalized received signal at that frequency.

The coefficients (C_k) are obtained from the channel frequency response, $H(f)$ based on either the Zero Forcing (ZF) criterion or the Minimum Mean Square Error (MMSE) criterion. The ZF criterion attempts to simply invert the channel where $H_k = H(k/T_s)$ is the channel frequency response at frequency $f_s = k/T_s$. The ZF criterion results in noise enhancement unless the signal-to-noise ratio (SNR) is high. This characteristic is in sharp contrast to the time domain equalizer where each tap coefficient is a function of the entire channel impulse response at all delays. The equalized signal is transformed back to time domain through application of the IDFT.

For high SNRs, CE OFDM performance in a frequency selective channel can be better than that in a flat fading channel when a frequency domain equalizer is employed due to the possibility of exploiting frequency diversity.

At the phase demodulator, the phase is extracted by taking the inverse tangent of the quadrature baseband components. This is followed by a phase unwrapper to obtain the demodulated phase. The phase estimate from the phase demodulator is confined to the 2π range from $-\pi \; to \; +\pi$. The original transmit phase that deviates outside the $-\pi \; to + \pi$ range is wrapped to within this range. Phase wrapping is more frequent for larger

modulation indices whereby the large OFDM signal peaks result in large fluctuations in the CE OFDM transmit phase.

The output of the phase demodulator is processed by the OFDM demodulator which consists of the N correlators, one corresponding to each subcarrier. This correlator bank is implemented in practice with the Fast Fourier Transform. The symbol de-mapper yields the received bits. The performance of the receiver improves if a finite impulse response filter is placed before the arctangent calculator [9, 11]. The performance is also dependent on the modulation index. The Symbol error rate is given by Eq. (22).

$$SER \approx 2\left(\frac{M-1}{M}\right) Q\left(2\pi h \sqrt{\frac{6log_2 M}{M^2-1}\frac{E_b}{N_0}}\right) \qquad (22)$$

Where Q is the Gaussian Q-function, E_b is the energy per bit of the transmitted bandpass CE OFDM signal and N_0 is the additive Gaussian noise [8]. The Bit Error Rate (BER) can be calculated as $BER \approx SER/log_2 M$.

III. 60 GHz CHANNEL CHARACTERIZATIONS AND MODELING

According to Shannon capacity theorem higher data rates demand very large transmission bandwidth. 60 GHz band is the huge unlicensed band where high data rate can be achieved. The 60 GHz wave exhibit strong atmospheric oxygen absorption (about 15dB/km) and high reflection. Fig. 4 shows the attenuation by oxygen and uncondensed water vapour as a function of frequency.

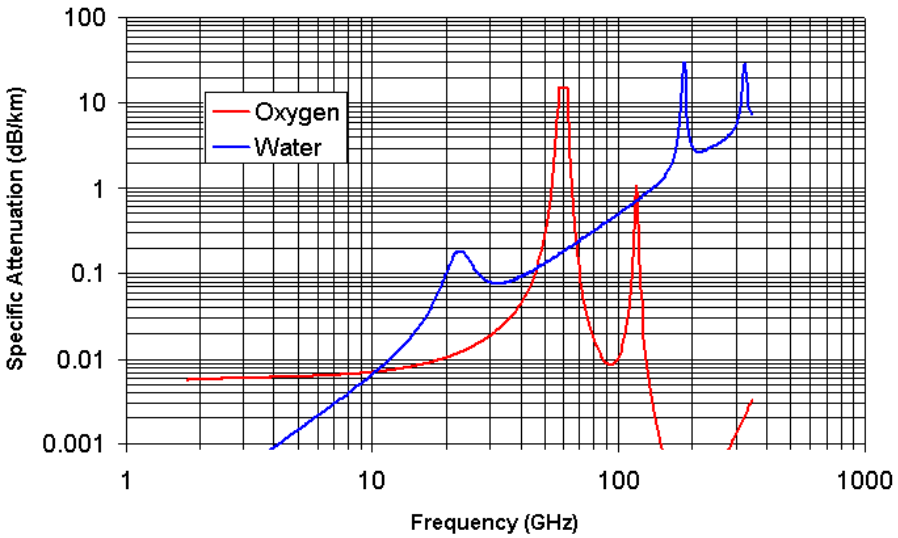

Fig. 4: Specific attenuation for atmospheric Oxygen and Water Vapour [28]

This high attenuation of the 60 GHz waves implies that cell radius will be few kilometres outdoor and in an indoor environment, the cell will be limited to a single room. Additionally concrete walls contribute to attenuation by 20 dB; this avoids interference with neighbouring cells. Absorption and reflection of electromagnetic wave are frequency dependent phenomenon. Everything which is larger than half the wavelength absorbs most of the power in the given direction and reflects the remaining. For 60 GHz wavelength is 5 mm, hence every object larger than 2.5 mm is an obstacle. To compensate atmospheric loss and reflection

loss higher antenna gain can be used without excessive antenna size. The influence of multipath interference can be reduced with use of narrow beamwidth antenna instead of omnidirectional one. But to provide better flexibility and link adaptability facilitating point-to-multipoint communications, moderate-directivity antennas or omnidirectional antennas are simple solutions in the design of 60 GHz wireless systems. [31]

SV Channel Model:

The Saleh–Valenzuela model [30] SV, is a very well-accepted statistical wideband channel model for indoor picocells. The channel model introduced concept of ray cluster, that is, multipath rays tend to reach the receiver in groups with similar delays, and angles of departure and arrival. These groups or clusters can be corresponding to reflections from same element such as a piece of furniture.

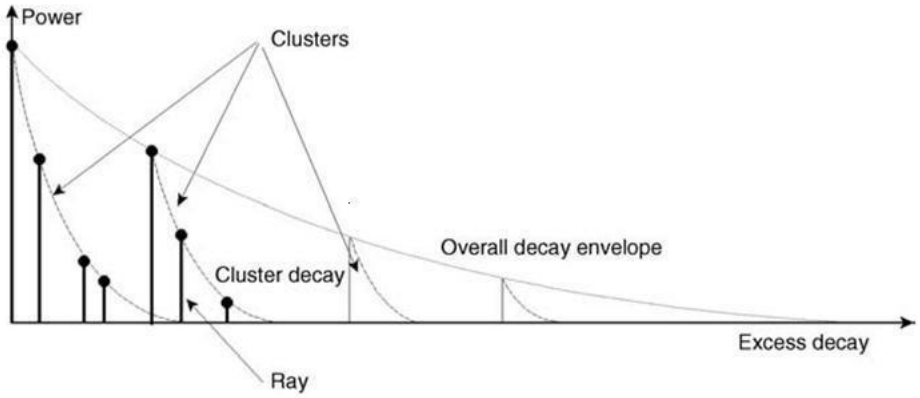

Fig. 5: A typical power delay profile based on the Saleh-Valenzuela model

Hence the overall channel impulse response can be expressed as

$$h(t) = \sum_{l}\sum_{k} \beta_{kl}\, e^{j\varphi_{kl}} \delta(\tau - T_l - \tau_{kl}) \qquad (23)$$

Where *l* indicates the cluster number and *k* indicates the ray number within a cluster. The amplitude (representing the received voltage) of each ray is β_{kl} Fig. 5. The received ray structure represents a decay rate defined by$\overline{\beta_{kl}^2}$,

$$\overline{\beta_{kl}^2} \equiv \overline{\beta^2(T_l, \tau_{kl})} = \overline{\beta^2(0,0)} e^{-T_l/\Gamma} e^{-\tau_{kl}/\gamma} \qquad (24)$$

Where $\beta^2(0,0)$ - the average power gain of the first ray of the first cluster,

Γ - Cluster power decay rate (envelope)

γ - Ray power delay rate within each cluster.

T_l - The cluster times of arrival

τ_{kl} - The ray times of arrival within cluster *l*

The number of arrivals and times of arrival for clusters and rays are characterized by Poisson and exponential distributions. The cluster arrival rate, *L*, denotes the inter-cluster arrival times, and the ray arrival rate, *l*, refers to the intra-cluster arrival times. The distributions of these arrival times are as follows,

$$p(T_l|T_{l-1}) = \Lambda exp[-\Lambda(T_l - T_{l-1})]$$

$$p(\tau_{kl}|\tau_{(k-1)l}) = \lambda exp[-\lambda(\tau_{kl} - \tau_{(k-1)l})] \qquad (25)$$

These two distributions are assumed to be independent of each other. Also the arrivals are conditioned or referred to the previous arrival.

The available literature on 60 GHz reports diverse findings for mean number of clusters. Analysis of IEEE 802.15.3c measurement data for various environments and scenarios shows that mean number of clusters does not follow a specific distribution. However, the observed mean number of clusters can be calculated by visual inspection. Values range typically from 3 to 14. The observed mean numbers of clusters are decided by measurement bandwidth and number of objects responsible for scattering.

IV. SIMULATION

A. Simulations Parameters

The system employed S-V channel model which describes the typical indoor transmission environment at 60 GHz. Channel parameters from IEEE 802.15.3c channel model at 60 GHz was used. The number of subcarriers used in OFDM system is 512, and the length of the cyclic prefix is 64. The modulation scheme used here is BPSK. All of the simulations assume that, channel-state information will not change in one OFDM symbol. To ensure the reliability of the computer simulations, OFDM symbols are generated to obtain each BER value in the simulations. The simulation is carried out for two channel models namely AWGN channel and SV channel model operating at 60 GHz.

For larger modulation index, the analytical expression becomes less accurate and for modulation index, h = 1.5, an irreducible error floor develops. The performance of CE OFDM system largely depends on the modulation index, h of the modulator. The spectral efficiency, S improves with modulation index but after certain value of modulation index the efficiency decreases [12]. The spectral efficiency can be calculated by the Eq. (17). The simulation is carried out for modulation index, $h=0.01$ that gives better spectral efficiency. This illustrates the limitation of discrete-time arctangent phase demodulator

B. Results

The comparison of CE OFDM and conventional OFDM for AWGN channel and for modulation index of the phase modulator $h=0.01$ is indicated in Fig. 6. It can be shown that *BER* decreases with increase in the modulation index, although those results were not included in this paper. Result shows that BER performance of conventional OFDM is better than CE OFDM for all SNR (signal to noise ratio) values. Here effect of large PAPR on power amplifier back off in case of conventional OFDM is not considered because for CE OFDM peak-to-average-power ratio is 0 dB. The result indicates that for any SNR value in the range of 0 to 35 dB conventional OFDM outperforms CE OFDM on the grounds of BER.

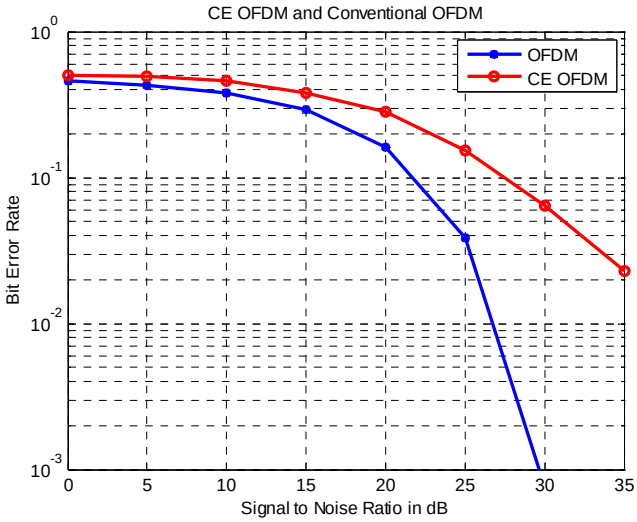

Fig. 6 Performance Comparison of CE OFDM and conventional OFDM

Same system is simulated at 60 GHz using SV channel model and various indoor scenarios were considered. It had been observed that change in the indoor scenario has relatively less effect on the BER of an OFDM

scheme. Fig. 7 compares BER performance of CE OFDM and conventional OFDM at 60 GHz frequency band using SV channel model and for modulation index of the phase modulator *h=0.01*

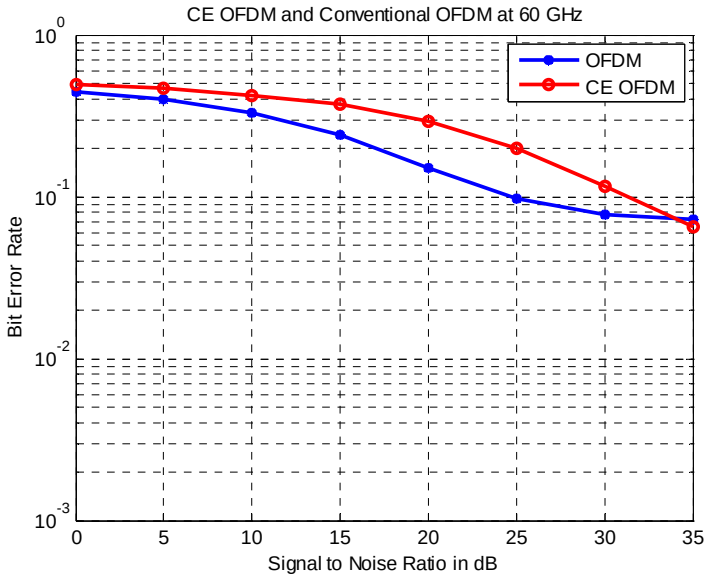

Fig. 7: CE OFDM and Conventional OFDM at 60 GHz (SV Channel Model)

Fig. 7 clearly indicates that difference in the BER of the two schemes for SV channel model is less as compared to the performance at AWGN channel. No doubt conventional OFDM outperforms CE OFDM at 60 GHz band also but at the cost of large PAPR while CE OFDM has 0 dB PAPR. Fig. 8 compares the performance of CE OFDM for AWGN channel and SV channel model working in 60 GHz band. It can be seen that system outshines for AWGN channel than at 60 GHz channel.

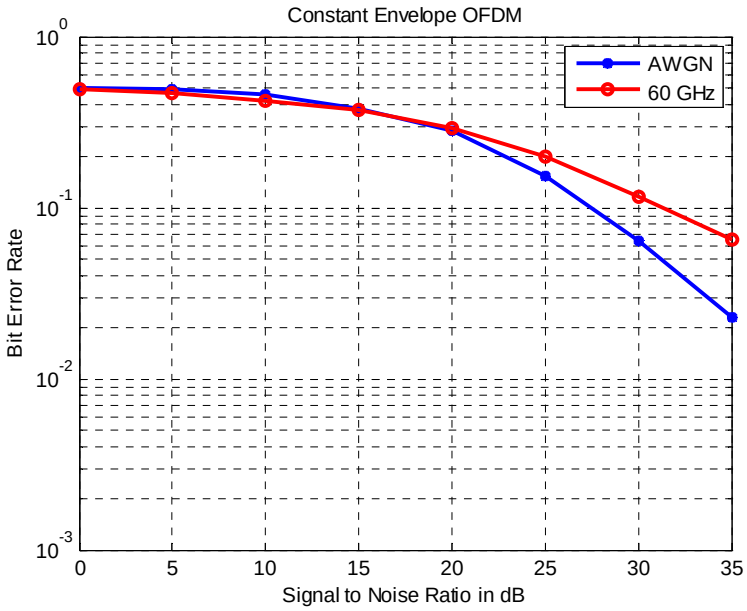

Fig. 8: CE OFDM for AWGN and at 60 GHz

V. CONCLUSION

The signal transformation technique used here eliminates PAPR by phase modulation. The phase modulation transforms the high peak-to-average ratio to *0* dB PAPR without any severe distortion. The simulation results show that CE OFDM compares favorably to conventional OFDM in multipath environment working the 60 GHz band. The system performance can be further enhanced with inclusion of efficient forward error correction technique.

The CE OFDM system demonstrates improved performance working in 60 GHz band as compared to AWGN channel. While conventional OFDM system degrades BER performance at 60 GHz compared to AWGN channel. The signal transformation technique reduces the high peak-to-average power ratio of conventional OFDM to nearly 0 dB; transforming it to Constant Envelope OFDM system. Particularly the bit error rate reduces with CE OFDM.

Conventional OFDM system suffers from inter modulation distortion and high amplitude variations which further degrades the performance of the system. These shortcomings are very well overcome in the CE OFDM system. CE OFDM suffers from the FM threshold effect. This problem can be solved with threshold extension techniques. Mostly, phase locked loops are known to reduce the threshold in FM systems by several dB. Realizing such an enhancement, and determining its complexity is very complex

REFERENCES

[1] C. E. Tan and I. J. Wassell, "Data bearing peak reduction carriers for OFDM systems", *IEEE Proceedings of the 2003 Joint Conference of the Fourth International Conference of Information, Communications and Signal Processing, 2003 and the Fourth Pacific Rim Conference on Multimedia*, Vol.2, 2003.

[2] H. Ahn, Y. M. Shin and S. Im, "A block coding scheme for peak to average power ratio reduction in an orthogonal frequency division multiplexing system", *IEEE Vehicular Technology Conference Proceedings*, Vol.1, 2000

[3] Christian Siegl and Robert F.H. Fischer, "Tone Reservation for Peak-to-Average Power Ratio Reduction in OFDM under Different Optimization Constraints", "*DFG*" within the framework *Take OFDM* under grant FI 982/1- 1

[4] D Matise, "*OFDM as a possible modulation technique for multimedia applications in the range of mm waves*", Introduction to OFDM, II edition, 10/30/98/TUD-TVS

[5] H. Ahn, Y. M. Shin and S. Im, "A block coding scheme for peak to average power ratio reduction in an orthogonal frequency division multiplexing system", *IEEE Vehicular Technology Conference Proceedings*, Vol.1, 2000

[6] H Liu and Guoqing Li, *OFDM-Based Broadband Wireless Networks: Design and Optimization*, A John Wiley & Sons, Inc., Publication, 2005

[7] J. G. Proakis, *Digital Communications*, 4th edition, New York: McGraw - Hill, 2001

[8] J. G. Proakis and D. G. Manolakis, *Digital Signal Processing: Principles Algorithms, and Applications*, 3rd edition, Upper Saddle River, New Jersey: Prentice Hall, 1996

[9] R. van Nee, R. Prasad, *OFDM for Wireless Multimedia Communications*, Boston, MA: Artech House, 2000, pp. 119-129

[10] R. W. Bauml, R. F. H. Fischer and J. B. Huber, "Reducing the peak to average power ratio of multi carrier modulation by selective mapping", *IEEE Electronics Letters*, Vol.32, 1996.

[11] R Van Nee, and A Wild, "Reducing the peak to average power ratio of OFDM", *IEEE Vehicular Technology Conference Proceedings*, Vol.3, 1998

[12] R. Prasad, *OFDM for Wireless Communications Systems*, Artech House, Inc. Boston, London, 2004

[13] S. H. Muller and J. B. Huber, "OFDM with reduced peak to average power ratio by optimum combination of partial transmit sequences", *IEEE Electronics letters*, Vol.33, 1997

[14] S. H. Muller and J. B. Huber, "A comparison of peak power reduction schemes for OFDM", in Proceedings of the IEEE Global Telecommunications Conference GLOBECOM '97, pp. 1-5, 1997

[15] S.C. Thompson, J. G. Proakis and J. R. Zeidler, "Constant Envelope Binary OFDM Phase Modulation", in *Proceedings of IEEE MILCOM*, Boston, 2003.

[16] S. C. Thompson, J. G. Proakis and J. R. Zeidler, "Non-coherent reception of constant envelope OFDM in flat fading channels," in *Proceedings of IEEE PIMRC*, Vol. 1, Berlin, 2005, pp. 517–521.

[17] S. C. Thompson, J. G. Proakis and J. R. Zeidler, "The effectiveness of signal clipping for PAPR and total degradation reduction in OFDM systems," in *Proceedings of IEEE Globecom*, Vol. 5, St. Louis, 2005, pp. 2807–2811

[18] S. C. Thompson, A. U. Ahmed, J. G. Proakis, J. R. Zeidler and M. J. Geile, "Constant Envelope OFDM", *IEEE Transactions on Communications*, Vol. 56, No. 8, 2008.

[19] S.C. Thompson, "Constant Envelope OFDM Phase Modulation," Ph.D. dissertation, University of California, San Diego, 2005. [Online]. Available: http://zeidler.ucsd.edu/~sct/thesis/

[20] S. C. Thompson, "Generating Real-Valued OFDM Signals with the Discrete Fourier Transform." [Online]. Available: http://zeidler.ucsd.edu/~sct/pubs/t5.pdf

[21] M. Kiviranta, A. M¨ammel¨a, D. Cabric, D. A. Sobel, and R. W. Brodersen, "Constant envelope multicarrier modulation: performance evaluation in AWGN and fading channels," in *Proc. IEEE Milcom*, vol. 2, Oct. 2005, pp. 807–813.

[22] A. R. S. Bahai, M. Singh, A. J. Goldsmith, and B. R. Saltzberg, "A new approach for evaluating clipping distortion in multicarrier systems," *IEEE J. Select. Areas Commun.*, vol. 20, no. 5, pp. 1037–1046, June 2002

[23] S. Sezginer and H. Sari, "OFDM peak power reduction with simple amplitude predistortion," *IEEE Commun. Letts.*, vol. 10, no. 2, pp. 65– 67, Feb. 2006

[24] M. Pauli and H.-P. Kuchenbecker, "Minimization of the intermodulation distortion of a nonlinearly amplified OFDM signal," *Wireless Personal Commun.* , vol. 4, no. 1, pp. 93–101, Jan. 1996.
[25] J. Armstrong, "Peak-to-average power reduction for OFDM by repeated clipping and frequency domain filtering," *IEE Electron. Lett.* vol. 38, no. 5, pp. 246–247, Feb. 2002.
[26] Peter Smulders, "Exploiting the 60 GHz Band for Local Wireless Multimedia Access: Prospects and Future Directions," *IEEE Communications Magazine* , January 2002
[27] P. F. M. Smulders, "Broadband Wireless LANs: A Feasibility Study," Ph.D. thesis, Eindhoven Univ. of Tech., The Netherlands, ISBN 90-386-0100-X, 1995; [Online]. Available: http://alexandria.tue.nl/extra3/proefschrift/PRF11B/95055 71.pdf
[28] *Millimetre Wave Propagation: Spectrum Management Implications*: Federal Communications Commission Office of Engineering and Technology, Bulletin Number 70, July, 1997.
[29] *TG3c Channel Modelling sub-Committee Final Report:* IEEE 802.15.3c contribution document, number: 15-07-0584-00-003c.
[30] A. A. M. Saleh, R. A. Valenzuela. "A statistical model for indoor multipath propagation," *IEEE J. Select. Areas Comm., SAC-5(2), 1987, 128–137.*
[31] Manabe, T., Miura, Y. and Ihara, T. (1996), "Effects of antenna directivity and polarization on indoor multipath propagation characteristics at 60 GHz," IEEE *J. Select. Comm.*, 441–8.